Astron. Astrophys. 118, 345–357 (1983)

ASTRONOMY AND ASTROPHYSICS

How to maintain the spatial distribution of interplanetary dust

C. Leinert[1], S. Röser[2], and J. Buitrago[3]

[1] Max-Planck-Institut für Astronomie, Königstuhl, D-6900 Heidelberg, Federal Republic of Germany
[2] Astronomisches Recheninstitut, Mönchhofstrasse, D-6900 Heidelberg, Federal Republic of Germany
[3] Instituto de Astrofisica de Canarias, C.S.I.C. Universidad de la Laguna, La Laguna, Tenerife, Spain

Received September 16, accepted October 28, 1982

Summary. We discuss two aspects related to the radial dependence of spatial density of interplanetary dust, which was found to be $n(r) \sim r^{-1.3}$ from the Pioneer 10/11 and Helios 1/2 space probes. Obviously, in steady-state a permanent source of dust is necessary to replenish the losses due to Poynting-Robertson effect and mutual collisions.

First, we ask which spatial distribution the dust source should have to lead to the observed *relative* spatial distribution. Sources limited to a shell at several AU heliocentric distance are found to be inadequate, while extended ($0.1\,\mathrm{AU} \leqq a \leqq 10\,\mathrm{AU}$ to 20 AU) sources with the semimajor axes distributed $\sim a^{-1.0}$ or $\sim a^{-1.1}$ reproduce the observed density gradient.

Second, we ask whether collisions in interplanetary space would destroy enough of the larger meteoroid particles to create a sufficient supply of dust-sized debris. This is found to be the case. In addition, the extended dust source resulting from these collisions approximately has the spatial distribution required to fit the observed radial dependence of dust density. We therefore consider radio and photographic meteoroids as the mass reservoir from which the interplanetary dust cloud is maintained.

Key words: interplanetary dust: spatial distribution – dynamics origin

1. Introduction

In order to maintain an equilibrium distribution of interplanetary dust in the presence of mass losses due to the Poynting-Robertson effect and mutual destructive collisions between the particles a continuous source of dust supply is needed. The required input was estimated to be $1\text{–}3\,10^4\,\mathrm{kg\,s^{-1}}$ over the whole mass range (Whipple, 1967; Dohnanyi, 1972). Generally, comets are considered as the initial source although a quantitative foundation for this hypothesis still is missing. Short period comets only are able to supply $70\text{–}250\,\mathrm{kg\,s^{-1}}$ (Delsemme, 1976; Röser, 1976).

During the last decade zodiacal light experiments on the Pioneer 10/11 and Helios 1/2 space probes have determined the radial distribution of interplanetary dust from 0.1 to 3 AU. The first task of our paper is to derive from these observations the relative spatial distribution of the required dust source. The result will be checked against the hypothesis that collisions between interplanetary particles provide an adequate input.

We consider as dust solid particles with radii less than 100 μm. Larger particles we call meteoroids, as usual. This somewhat arbitrary separation of the smooth size distribution of interplanetary particles is made for the ease of presentation and, more importantly, because the zodiacal light observations almost exclusively refer to the size range of interplanetary dust. In fact, about 95% of the zodiacal light is due to particles with radii less than 100 μm (Röser and Staude, 1978), which shows that meteoroids virtually are not covered by zodiacal light observations. A further distinction comes from the dynamics of the particles. Collisions are dominating the lifetimes of meteoroids while dust particles mainly are subject to the Poynting-Robertson effect.

The second task of our paper is to check whether collisions between interplanetary particles could provide a dust input large enough to maintain the observed spatial density in steady-state. We visualize this input as being due to the disruption of larger particles, the debris of which largely would be in the size range of dust. This input has to be large enough to cancel the dust losses due to Poynting-Robertson effect as well as the losses of submicron particles which are driven out of the solar system as β-meteoroids by radiation pressure.

We do not try to explain how the larger particles are being supplied and what actually constitutes the primary source of solid interplanetary material.

We add several remarks concerning the first task of our paper.

As reference to which our model calculations of relative spatial distribution have to be compared we adopt the relation $n(r) \sim r^{-1.3}$ measured by Helios (Leinert et al., 1981) inside 1 AU. Based on the geometry of the Helios measurements one expects that the same power law should be valid out to at least 1.5 AU. From Pioneer observations Hanner et al. (1976) proposed a slightly different spatial distribution outside 1 AU, $n(r) \sim r^{-1.5}$ with an enhancement in the asteroid belt and a cut-off at 3.3 AU. Figure 1 shows that both curves have the same average trend. Also both represent the observed zodiacal light brightnesses quite well. We then prefer to use the extension of the power law from the inner solar system since we will see later that the assumption of an enhancement in the asteroid belt is not really justified. According to Schuerman (1980) the Pioneer data support a steeper decrease of spatial density with heliocentric distance but his argument appears to concern only the region outside 2 AU. Therefore we take as best description of the spatial distribution simply the above power law $n(r) \sim r^{-1.3}$, with a stronger decrease setting in somewhere between 2 and 3.3 AU. Doing so we neglect the results of the meteoroid penetration detectors on Pioneer 10 and 11, which were interpreted by constant spatial density of interplanetary dust out to 18 AU (Humes, 1980). We suggest to postpone a discussion of this discrepancy until new measurements from the forthcoming space probes to Jupiter become available. Inside

Send offprint requests to: C. Leinert

1 AU zodiacal light measurements and particle detection experiments are compatible (Grün et al., 1977).

We are aware of three previous attempts to explain the radial distribution of interplanetary dust, none of which is in quantitative agreement with the above observations. Briggs (1962) considered the effect of Ponyting-Robertson drag on an extended source of dust, distributed like the photographic meteors selected by Hawkins and Southworth (1961). He finds a slope of $r^{-1.0}$ inside 1 AU which steepens to about r^{-3} near 4 AU. Southworth (1967), assuming instead particles in initially highly eccentric orbits, arrived at a similar result. Trulsen and Wikan (1980) suggested that inelastic collisions between dust particles might reduce their average inclination, when, under the action of the Poynting-Robertson-effect, they are drifting towards the Sun. This also would lead to a steepening of the dust distribution in the ecliptic plane.

Under the action of the Poynting-Robertson effect alone the spatial distribution of interplanetary dust will tend towards $n(r) \sim 1/r$ inside the source region. This is the limiting case. Smaller slopes cannot be obtained without an additional loss mechanism. We want to explain a steeper slope. Such a distribution will be obtained in an extended source region, because the addition of new material to the inward drifting outer particles steepens the spatial distribution all over the source region. This is our basic idea for explaining the relative spatial dust distribution. How large the deviation from the limiting $1/r$-law will be depends on how strongly the dust input increases towards the Sun. Our approach therefore is similar to Briggs' (1962), but we also include a discussion of the effect of collisions.

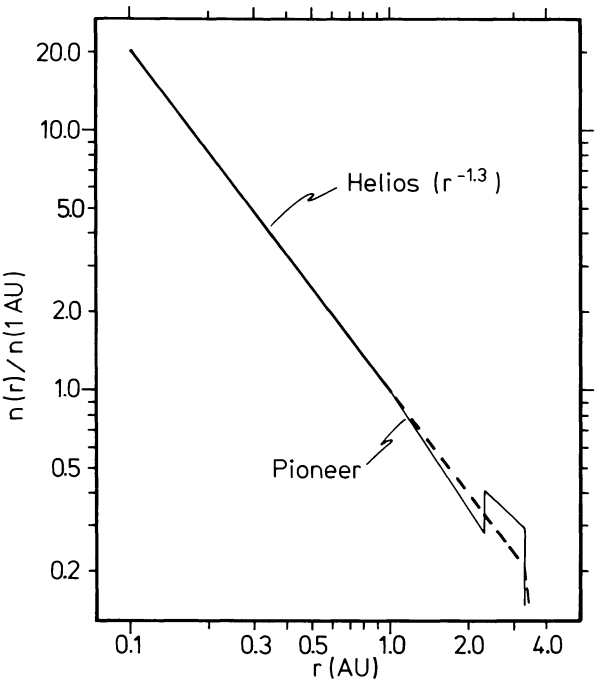

Fig. 1. Observed radial distribution of interplanetary dust. Outside 1 AU the interpretation is not unique. An extension of the power law (– – –) is the simplest acceptable choice

2. Formulation of the problem

2.1. The continuity equation

We assume the zodiacal cloud to be in steady-state and cylindrically symmetric. The system is described by the orbital parameters a (semimajor-axis), e (eccentricity), and i (inclination), and by the particle radius s. Longitude of ascending node and of perihelion are assumed to be randomly distributed. The size distribution is taken as independent of the spatial density; this simplification is not in contradiction with the observations. For a statistical formulation of the problem, we use the following notations:

N_T Total number of particles (constant in time)

N^i Total number of particles injected per unit of time (constant in time)

$N_T \cdot f(a,e,i) \cdot g(s) da de di ds$ Number of particles having orbital parameters in the range $(a, a+da)$, $(e, e+de)$, $(i, i+di)$ and radii in the range $(s, s+ds)$.

The distribution function $f^i(a,e,i) \cdot g^i(s)$ of the injected particles is similarly defined. The functions f, f^i and g, g^i are normalized to 1.

In (a, e, i)-space the vector denoting the secular changes of orbital parameters is

$$\boldsymbol{u} = \left(\frac{da}{dt}, \frac{de}{dt}, \frac{di}{dt}\right). \tag{1}$$

In steady-state, for each particle radius s the net flux of particles per unit volume in (a,e,i)-space is counterbalanced by the rate of injection minus destruction by collisions

$$\mathrm{div}[\boldsymbol{u} N_T f(a,e,i) \cdot g(s)] = N^i f^i(a,e,i) g^i(s) + \left[\frac{\partial N(a,e,i,s)}{\partial t}\right]_{\mathrm{coll}}, \tag{2}$$

where $\mathrm{div} = \left(\frac{\partial}{\partial a}, \frac{\partial}{\partial e}, \frac{\partial}{\partial i}\right)$ by definition.

Lorentz force and Coulomb drag are neglected, which seems permissible, since most of the zodiacal light is due to comparatively large particles with radii 10–100 μm (Röser and Staude, 1978).

Collisions destroy particles; at the same time they also produce a debris of smaller particles. The collision term in Eq. (2) is only covering the losses due to collisions, i.e. it gives the rate at which particles of a given radius are being destroyed per unit volume in (a,e,i)-space. Dust production by collisions is *not* included in our collision term, but incorporated into the source function f^i together with all other contributing processes. The treatment of collisions is described in Sect. 2.3. The collision term then may be written as

$$\left[\frac{\partial N(a,e,i,s)}{\partial t}\right]_{\mathrm{coll}} = -N_T \cdot f(a,e,i) \cdot g(s) \frac{1}{\tau_c(a,e,s)}, \tag{3}$$

where τ_c is the size-dependent lifetime against collisions. The relative brightness *distribution* of the zodiacal light as observed by Helios (Leinert et al., 1981) shows no appreciable change between 1.0 and 0.3 AU. This supports a factorization

$$f(a,e,i) = f_1(a,e) \cdot f_2(i) \tag{4}$$

of the steady-state distribution. This condition then automatically holds for the input distribution, because the radiation forces alone do not change the inclination of a particle orbit and other forces are not considered. Equation (2) now becomes

$$\mathrm{div}[\boldsymbol{u} N_T f_1(a,e)] = N^i f_1^i(a,e) \frac{g^i(s)}{g(s)} - N_T f_1(a,e) \frac{1}{\tau_c(a,e,s)}. \tag{5}$$

On the left hand side of the equation we adopt the well known expressions for the secular changes of a, e, i due to Poynting-

Robertson effect (Robertson, 1937; Wyatt and Whipple, 1950):

$$\frac{da}{dt} = -\alpha \frac{2+3e^2}{a(1-e^2)^{3/2}}, \quad \frac{de}{dt} = -\frac{5\alpha e}{2a^2(1-e^2)^{1/2}}, \tag{6}$$

where

$$\alpha = \frac{3\cdot 55\,10^{-8}\cdot Q_{pr}}{s(\mathrm{cm})\cdot \varrho(\mathrm{g\,cm^{-3}})} \quad (\mathrm{AU})^2/\mathrm{yr}.$$

Q_{pr} is the efficiency factor for radiation pressure. For our purpose to explain features of the spatial density distribution, it is in order to work with the simple expression for perfectly absorbing particles, $Q_{pr} = 1.0$.

Evaluation of Eq. (5) using the derivatives given in (6) gives the equation describing our problem:

$$N_T\left[\frac{\partial f_1(a,e)}{\partial a}\cdot\frac{\alpha(2+3e^2)}{a(1-e^2)^{3/2}} + \frac{\partial f_1(a,e)}{\partial e}\cdot\frac{5\alpha e}{2a^2(1-e^2)^{1/2}}\right]$$
$$= N_T\frac{\alpha(6e^2-1)}{2a^2(1-e^2)^{3/2}} f_1(a,e) - N^i f_1^i(a,e)\frac{g^i(s)}{g(s)}$$
$$+ N_T f_1(a,e)\frac{1}{\tau_c(a,e,s)}. \tag{7}$$

2.2. Particle size distribution

The particle size distribution $g^{(i)}(s)$ is a sensitive parameter in our calculations. Obviously, the probability of an individual particle to collide, and hence its lifetime, linearly depends on $g(s)$. The number of collisions per second and with it the rates of mass loss and creation of collisional products depend on $g^2(s)$. We adopted for $g(s)$ the "maximum model" of Giese and Grün (1976) in the numerical form given by Fechtig et al. (1981), because it appears to us well founded experimentally and reproduces zodiacal light intensities for a reasonable dust albedo of ≈ 0.2 (Hanner, 1980). This distribution is shown in Fig. 2 together with two other proposed size distributions. The distribution of LeSergeant and Lamy (1980), like the "maximum model" is based on microcrater counts on lunar rocks. Future discussions will have to show, which of the two size distributions is more reliable. Cook's (1978) result mainly is based on observations of faint optical meteors. It appears too high to us, requiring a very low albedo of 0.006 at 1 AU to fit it to the zodiacal light observations. It will be used only to demonstrate the influence of size distribution. Generally we will assume the same spatial distribution $n \sim r^{-1.3}$ for all particle sizes, i.e. the same size distribution at all heliocentric distances. This simple picture may have to be modified, since Southworth and Sekanina (1973) obtained a quite different spatial distribution for radio meteoroids, with a large excess in the range 1–4 AU. The implications of this modification will be discussed at those places where they are relevant.

2.3. Collisional model

The effect of collisions on particles in the size range 1–100 μm is twofold. By destroying such particles they constitute a loss mechanism to the interplanetary dust cloud; by fragmentating larger bodies they create a source of interplanetary dust. An expression for the losses is needed for the continuity equation. The source will be compared with the required input.

For our calculations we use the simple model of Dohnanyi (1978) with a few additional simplifications. Since Dohnanyi (1972) as well as Le Sergeant d'Hendecourt and Lamy (1981) showed that in interplanetary space catastrophic collisions, i.e. collisions which disrupt the colliding particles, are dominant, we neglect erosive collisions. We also take all particles as spherical and of same specific density ϱ.

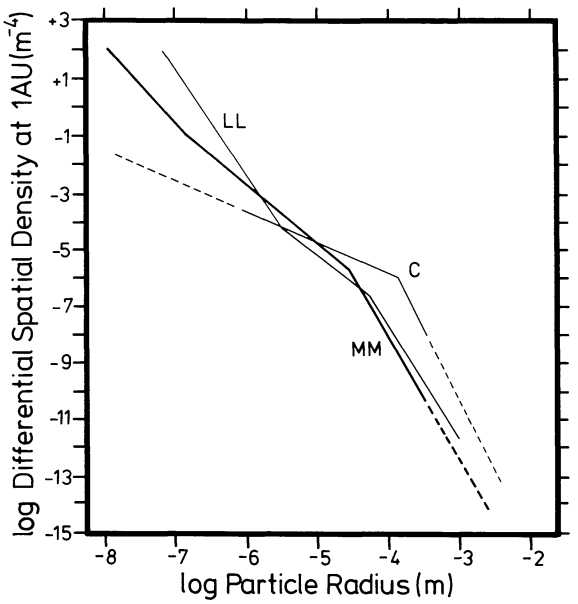

Fig. 2. Particle size distributions of interplanetary dust at 1 AU. MM: "maximum model" by Giese and Grün (1976). LL: Le Sergeant d'Hendecourt and Lamy (1980). C: Cook (1978)

A catastrophic collision is assumed to occur if two particles touch and if the mass of the projectile (radius s') is not too small with respect to the target (radius s), i.e.

$$s'^3 \geqq \frac{1}{\Gamma} s^3, \tag{8}$$

where Γ was found experimentally to vary with v^2. For an impact velocity of $v = 10\,\mathrm{km\,s^{-1}}$, which is typical in interplanetary space at 1 AU, simulation experiments predict $\Gamma \approx 5\,10^4$ (Grün, 1981). The size distribution of the fragments was found in laboratory experiments to be

$$j(s_1) = C(s)\cdot s_1^{-3.4} \tag{9}$$

(Dohnanyi, 1978; Fujiwara et al., 1977), where $C(s)$ is determined by the conservation of mass requirement

$$\int_0^{\lambda s} \frac{4\pi}{3}\varrho s_1^3 ds_1 = \frac{4\pi}{3}\varrho s^3. \tag{10}$$

λs is the size of the biggest fragment which we took to have 1/50 of the mass of the target particle. Since we do not intend to study the size distribution of collisional products this simplification with respect to Fujiwara et al.'s (1977) formula seems acceptable.

The collision frequency of an interplanetary particle at heliocentric distance r is

$$\frac{1}{\tau_c(r,s)} = n(r)\cdot\langle v\sigma\rangle_{a',e'}, \tag{11}$$

where the averaging extends over all orbits of projectile particles which pass through the position of the target particle, i.e. with $a'\cdot(1-e') \leqq r \leqq a'(1+e')$. The relative velocity of the colliding particles, $v(r,a,e,a'e')$, also is a function of the orbital parameters $a, e,$

of the target particle, but in the average the expression simplifies to

$$\frac{1}{\tau_c(r,s)} = n(r)\langle v(r)\rangle \int_{s/\Gamma^{1/3}}^{\infty} \pi(s+s')^2 g(s')\,ds'. \tag{12}$$

$\langle v(r)\rangle$ is assumed to vary like Keplerian orbital velocities,

$$\langle v(r)\rangle = v(r_0)\cdot(r/r_0)^{-0.5}, \tag{13}$$

where $r_0 = 1$ AU is used as reference distance from the Sun. The integral in (12) gives the average cross-section σ_{cc} of the target particle for a catastrophic collision to occur with the passing projectile particles. Because of the velocity dependence of Γ its value increases towards the Sun, where the higher orbital velocities allow smaller projectiles to destroy a given target. We calculated for the size distribution of Giese and Grün (1976) the dependence of σ_{cc} on Γ, which because $\Gamma \sim v^2$ directly translates into the dependence on heliocentric distance. In the target size range 10–60 μm, which is most important for zodiacal light, the dependence turned out to be a power law with exponent 0.23–0.28. For ease of the following calculations we approximated this by

$$\sigma_{cc}(r) = \sigma_{cc}(r_0)\cdot(r/r_0)^{-0.2}. \tag{14}$$

The loss of particles by collisions at a given heliocentric distance is

$$L(r,s) = -\frac{n(r)g(s)}{\tau_c(r,s)}, \tag{15}$$

the gain

$$G(r,s_1) = n(r)s_1^{-3.4}\int_{s/\lambda}^{\infty} \frac{g(s)C(s)}{\tau_c(r,s)}\,ds \tag{16}$$

particles per unit volume per second per unit size interval. In these formulae each particle enters twice, once as target, once as projectile, but is only counted once. Conservation of mass requires

$$\int_0^{\infty} \frac{4\pi}{3}\varrho s^3[G(r,s)-L(r,s)]\,ds = 0, \tag{17}$$

which we used to check our calculations.

2.4. The collision term in the continuity equations

To obtain the collisional probability for a particle having orbital parameters, a, e we have to average (12) over the range of distances covered by this particle,

$$\frac{1}{\tau_c(a,e,s)} = \int_{r=a(1-e)}^{a(1+e)} W(r)\frac{1}{\tau_c(r,s)}\,dr. \tag{18}$$

$W(r)dr$ gives the probability for the particle to be in the spatial interval $(r, r+dr)$.

An interplanetary particle most probably will collide with one of the more numerous particles smaller than its own size. As far as we are considering the lifetimes of dust it therefore is safe to use in (12) the spatial distribution

$$n(r) = n(r_0)(r/r_0)^{-1.3} \tag{19}$$

valid for the particles producing the zodiacal light, even if meteoroids should have a different spatial distribution. By the same reasoning, (19) still would be a reasonable approximation, at least for the smaller ones among the meteoroids. Inserting the dependence with heliocentric distance for n, v, σ, we obtain from (18)

$$\frac{1}{\tau_c(a,e,s)} = n(r_0)v(r_0)\sigma(r_0)\int_{r=a(1-e)}^{a(1+e)} W(r)(r/r_0)^{-2.0}\,dr, \tag{20}$$

where

$$n(r_0)v(r_0)\sigma(r_0) = \frac{1}{\tau_c(r_0,s)}$$

is the collision probability (s^{-1}) of a particle at $r_0 = 1$ AU. The integral in (20) is the time average of $1/r^2$ over one particle orbit, which may be evaluated using Kepler's second law to give

$$\frac{1}{\tau_c(a,e,s)} = \frac{1}{\tau_c(1\text{ AU},s)}\cdot\frac{(1\text{ AU})^2}{a^2(1-e^2)^{1/2}}. \tag{21}$$

This has to be compared with the lifetime against Poynting-Robertson effect which was given as

$$\tau_{PR}(r,s) = \frac{r^2}{4\alpha} \tag{22}$$

by Wyatt and Whipple (1950) for a particle in circular orbit. We will see below that not the collision lifetime itself but the ratio of collision lifetime to Poynting-Robertson lifetime is important for the relative spatial distribution of interplanetary dust. Because of (14), both lifetimes have the same dependence on heliocentric distance, and it is sufficient to calculate τ_{PR}/τ_c at 1 AU.

3. Solution of the continuity equation

3.1. Equilibrium distribution and spatial density

Equation (7) with expression (21) is a partial linear differential equation of first order which can be treated by standard mathematical methods, once the source function $f_1^i(a,e)$ is specified.

For solving Eq. (7), it is necessary to find two independent integrals of the associated system of characteristics

$$\frac{a(1-e^2)^{3/2}da}{\alpha(2+3e^2)} = \frac{2a^2(1-e^2)^{1/2}de}{5\alpha e},$$

$$\frac{2a^2(1-e^2)^{1/2}de}{5\alpha e} = \frac{df_1}{\left[\dfrac{\alpha(6e^2-1)}{2a^2(1-e^2)^{3/2}} + \dfrac{r_0^2}{\tau_c(r_0,s)a^2(1-e^2)^{1/2}}\right]f_1 - \dfrac{N^i}{N_T}\cdot f_1^i(a,e)\dfrac{g^i(s)}{g(s)}}. \tag{23}$$

The first integral turns out to be the relation obtained by Wyatt and Whipple (1950)

$$\frac{e^{4/5}}{a^2(1-e^2)} = \text{const}, \tag{24}$$

which determines the orbital evolution of particles released at some starting point (a_0, e_0).

To obtain the second integral we first solve the homogeneous part of the second Eq. in (23), which results in

$$f_1(a,e) = \text{const}(1-e^2)^{-1/2}\exp(-\tfrac{1}{5} + 2r_0^2/5\alpha\tau_c). \tag{25}$$

Then a particular solution $f_1(a,e,f_1^i)$ is constructed by the method of the variation of the constant. It turns out that for adequate

boundary conditions [e.g. $f_1(a,e)\to 0$ for $a\to\infty$, $f_1(a,e)\equiv 0$ if $f_1^i(a,e)\equiv 0$] the possible additional terms disappear and we just are left with our particular solution.

$$N_T f_1(a,e)g(s)=\frac{2N^i}{5\alpha(1-e^2)^{1/2}e^{1/5}}\cdot\int_{\tilde e=e}^{e_{\max}} f_1^i(\tilde a,\tilde e)g^i(s)\tilde a^2\tilde e^{-4/5}(1-\tilde e^2)\cdot\exp\left[-\frac{2r_0^2}{5\alpha\tau_c(r_0,s)}\log\frac{\tilde e}{e}\right]d\tilde e. \tag{26}$$

Here the integral is along that curve in a,e-space, which is determined by the Poynting-Robertson drift (24). Equation (26) can be interpreted as follows. The steady-state value of the distribution function f_1 at a point (a,e) is computed by adding up all contributions from the input distribution which eventually may pass through position (a,e). The factor $\exp\left[-\frac{2}{5}\frac{r_0^2}{\alpha\tau_c(r_0,s)}\log\frac{\tilde e}{e}\right]$, short $P(\tilde a,\tilde e\to a,e)$, is the probability of a particle to survive the drift from point $(\tilde a,\tilde e)$ to point (a,e) without suffering a collision. In a sense, Eq. (26) needs iteration because to calculate τ_c or that part of f^i which is produced by collisions, we already need knowledge of the steady-state distribution. However, as long as we do not try a fully self-consistent solution, but consider τ_c and f^i as parameters for which reasonable choices have to be made, this problem does not occur. Using (22), the probability of survival can be written as

$$P(\tilde a,\tilde e\to a,e)=\exp\left[-\frac{8}{5}\frac{\tau_{PR}(r_0,s)}{\tau_c(r_0,s)}\log\frac{\tilde e}{e}\right]. \tag{27}$$

As expected the probability of survival essentially depends on the ratio of the two timescales, τ_{PR}/τ_c. For illustration Fig. 3 shows survival probabilities of a particle starting at $a=4$ AU with $e=0.5$ for different values of the ratio τ_{PR}/τ_c. Finally, replacing the integration variable $\tilde e$ in (26) by $\tilde a$ via (6) one arrives at

$$N_T f_1(a,e)\cdot g(s)=\frac{N^i}{\alpha a^{1/4}(1-e^2)^{3/4}}\cdot\int_{\tilde a=a}^{a_{\max}} f_1^i(a,e)g^i(s)\tilde a^{5/4}\frac{(1-\tilde e^2)^{9/4}}{2+3\tilde e^2}\cdot\exp\left[-\frac{\tau_{PR}}{\tau_c}\log\frac{\tilde a^2(1-\tilde e^2)^2}{a^2(1-e^2)^2}\right]d\tilde a, \tag{28}$$

which has been used for numerical integration applying (24) for the calculation of $\tilde e$ as a function of $\tilde a$.

Once the steady-state distribution is known, the spatial density is given by Haug (1958) as

$$n(r,\beta)g(s)=\frac{N_T}{2\pi^3 r\cos\beta}\iiint_{a\,e\,i}\frac{f(a,e,i)\cdot g(s)\,da\,de\,di}{r^2\left(\frac{a}{r}\right)^{3/2}\left[2-\frac{r}{a}-\frac{a}{r}(1-e^2)\right]^{1/2}[\sin^2 i-\tan^2\beta\cos^2 i]^{1/2}}, \tag{29}$$

where r and β denote the radial distance from the Sun and the heliocentric ecliptic latitude of the volume element under question. With the help of (4) we can write $n(r,\beta)=n_1(r)\cdot n_2(\beta)$, with

$$n_1(r)=\frac{N_T}{2\pi^3}\cdot\frac{1}{r}\int_{a=\frac{r}{1+e}}^{\frac{r}{1-e}}\int_{e=0}^{1}\frac{f_1(a,e)\,de\,da}{a^2\left[e^2-\left(\frac{r}{a}-1\right)^2\right]^{1/2}},\qquad n_2(\beta)=\int_{i=\beta}^{\pi/2}\frac{f_2(i)\,di}{[\sin^2 i-\sin^2\beta]^{1/2}}. \tag{30}$$

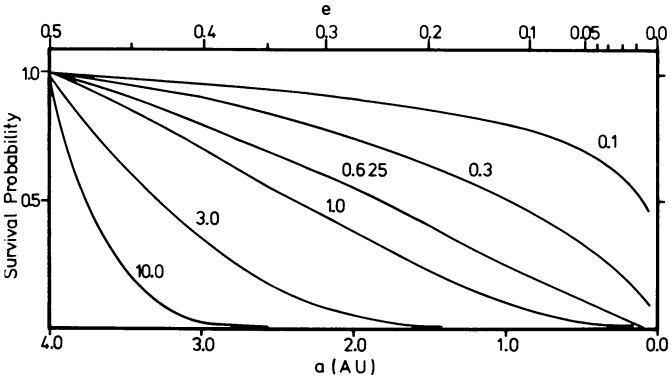

Fig. 3. Survival probabilities of a particle, starting at $a=4$ AU with an eccentricity of $e=0.5$, for different values of the ratio τ_{PR}/τ_c. The respective values of this ratio are indicated on each curve. Example: If $\tau_{PR}/\tau_c=0.1$ the particles has a 50% chance to reach 0.1 AU, while for $\tau_{PR}/\tau_c=10$ the chance to reach 3 AU only is 3%

In Sect. 4 we will compute $n_1(r)$ for different input functions $f_1^i(a,e)$ and compare with the observed spatial distribution of interplanetary dust.

3.2. *An analytical result*

Under certain conditions the relations between the spatial density $n(r)$, the steady-state distribution $f_1^i(a,e)$ can be found analytically. Let us assume

$$f_1^i(a,e)\sim a^x\cdot h^i(e), \tag{31}$$

with $x<-1$ to have a finite total input. Using (24) we can replace $\tilde a$ by a in (26). Then it is easy to see that

$$f_1(a,e)\sim a^{x+2}\cdot h(e). \tag{32}$$

The reverse is also true, as follows directly from the differential equation (7) since $\tau_c\sim a^2$ in our collisional model. We would like to stress that these relations hold both in the case with and without collisions. Moreover, if collisions are highly dominant, $\tau_{PR}/\tau_c\gg 1$, then $\alpha\ll 1/\tau_c$ and we obtain the above relationship in greater generality,

$$f_1(a,e)\sim\tau_c(a,e)\cdot f_1^i(a,e). \tag{33}$$

Since a steady-state distribution of the form (32) leads to a spatial distribution

$$n(r)\sim r^x \tag{34}$$

(Bandermann, 1967), we have the simple result that an input distribution proportional to a power law in semimajor axis (31) leads to a spatial distribution which is given by the same power law as function of r. This analytical result strictly is valid only if the input region is unlimited, but it may serve as a guideline for estimating the results for finite input distributions.

4. Numerical results

4.1. *Calculation*

From Eqs. (28) and (30), the spatial density at distance r can be obtained for a given input distribution by triple integration over

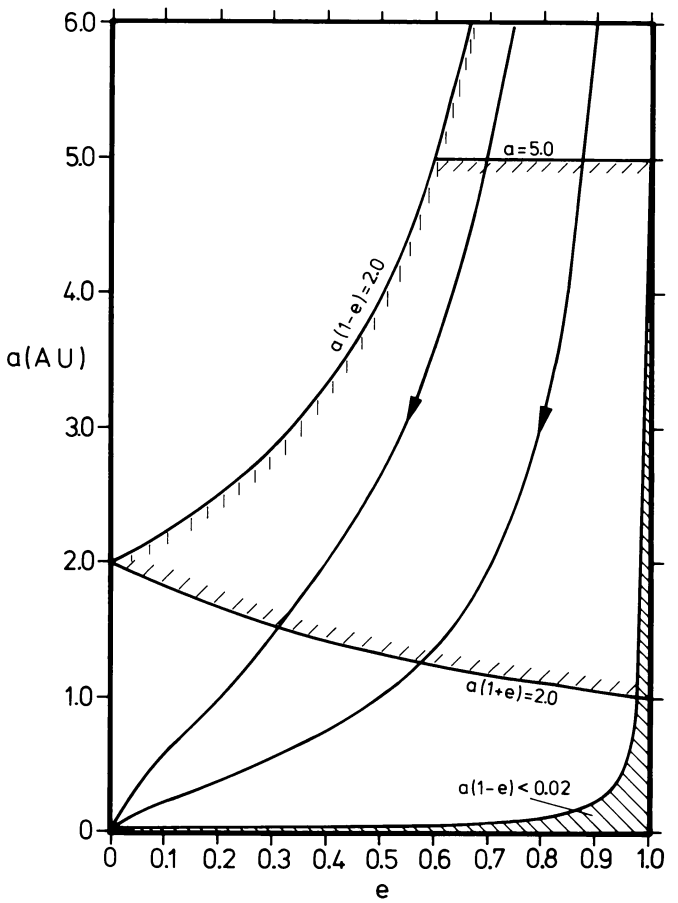

Fig. 4. Integration limits for calculating the spatial density at $r=2$ AU with an input limited to particles with semimajor axes $a \leqq 5$ AU

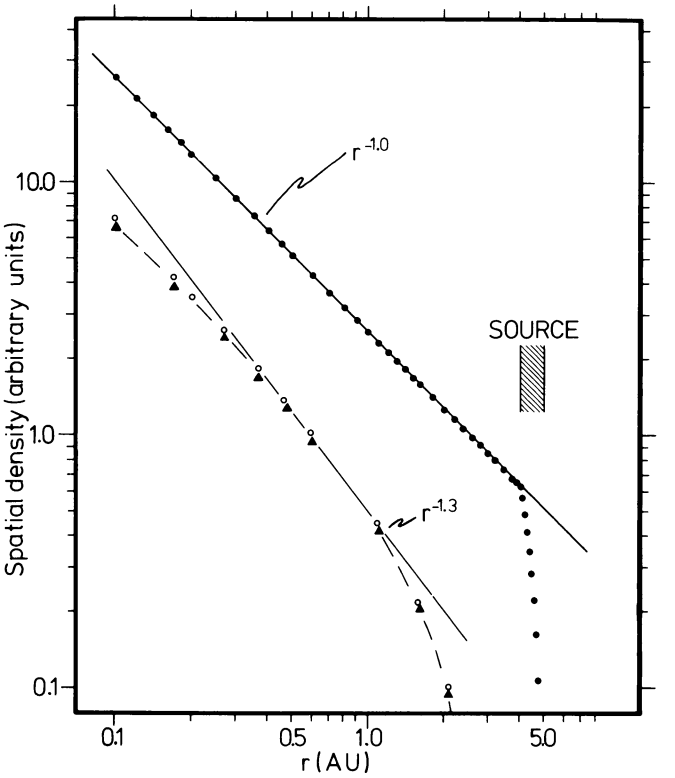

Fig. 5. Spatial distribution resulting from an external source of particles in ● circular orbits, source in the region 4–5 AU; ○ same source region, but eccentricity distribution $h'(e) \sim e \cdot \exp(-2e^2)$; ▲ highly eccentric orbits, $\bar{e}=0.9$, source in the region 9–20 AU

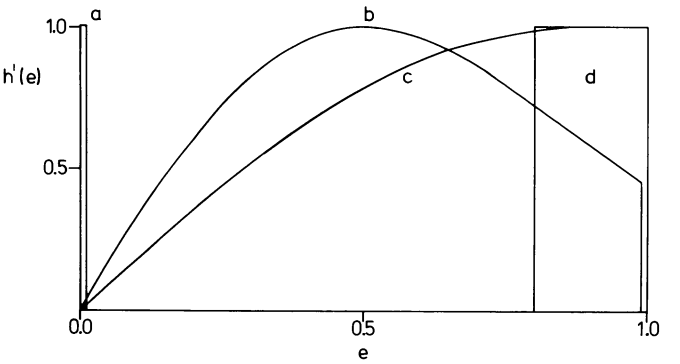

Fig. 6. Various distributions of eccentricity. *a* "circular" orbits, $\bar{e}=0.005$; *b* and *c* Rayleigh distributions with maxima at $e=0.5$ and $e=0.9$, $\bar{e}=0.53$ and 0.62; *d* highly eccentric orbits, $\bar{e}=0.9$; not shown: equally distributed eccentricities, $\bar{e}=0.5$. Note that the distributions are normalized to a maximum value of 1.0

a, e, and $\tilde{a}$. Figure 4 helps to visualize the integration limits involved. The area in the a-e-plane, for which values of the steady-state-distribution $f_1(a, e)$ have to be calculated is determined mainly by the requirement that the aphelion of the particles be larger and the perihelion smaller than the chosen distance r. Additional constraints are given by the evaporation of the particles, assumed to occur instantaneously for perihelia less than 0.02 AU, and by the upper limit of semimajor axis adopted for the respective input distribution. For each of the remaining points the steady-state value of $f_1(a, e)$ is obtained, according to Eq. (28), by integration back along the path which leads the inward drifting particles to the specific point. Two typical paths are included in Fig. 4. The integration was done according to the trapezoidal rule. The integrand in (30) is not bound at the limits of the integration over a, but this part can be evaluated analytically. After checking the influence of step size we did the numerical integrations mostly with 15 steps in a, 40 steps in e and steps of 0.05 AU along the drift curves which typically leads to an accuracy of better than 1%. The integration steps were refined where necessary for particular input functions.

4.2. *Models neglecting collisional losses*

a) Tests and choice of eccentricity distribution

The tests included checks of the program by repetition of calculations with known analytical results and calculations concerning the influence of particle orbit eccentricity.

The example in Fig. 5 shows that an external source of particles in circular orbits indeed leads to a spatial distribution $n(r) \sim 1/r$. Contrary to naive expectation the density in the source region is particularly low.

Particles in eccentric orbits initially have a higher drift rate than particles in circular orbits of the same semimajor axis. As the eccentricity decreases, the difference in drift velocity disappears, leading to a steeper spatial distribution $n(r)$ than obtained for circular orbits. However, it was not possible to reproduce the observed spatial distribution by a shell source of particles with eccentric orbits at larger heliocentric distance. The resulting

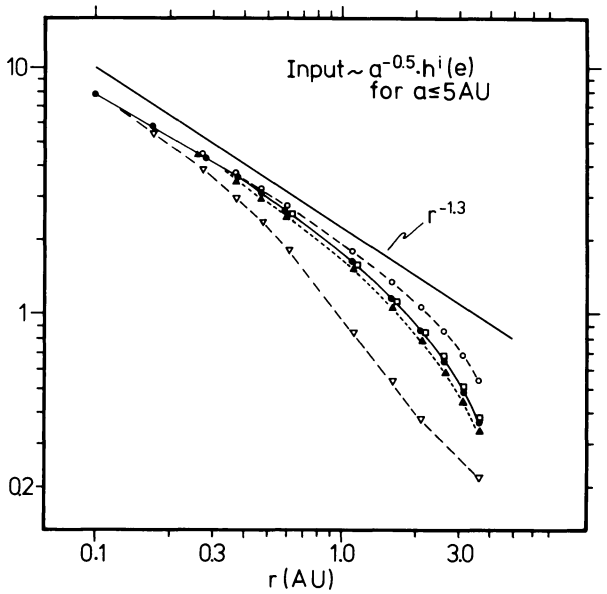

Fig. 7. Influence of eccentricity distribution of the source particles on the resulting spatial distribution. Curves have been normalized at 0.1 AU. Average eccentricities are 0.005 (○), 0.5 (□), 0.53 (●), 0.62 (▲), 0.9 (▽)

spatial distribution $n(r)$ is curved, e.g. the slope is too small in the inner and too large in the outer region (Fig. 5).

The effect of eccentricity on *extended* sources is given in Fig. 7 for the case where the input is limited to particles with semimajor axis $a \leqq 5.0$ AU and the input distribution is proportional to $a^{-0.5}$. Distributions with average eccentricities between 0.005 and 0.9 were considered (Fig. 6). The influence of eccentricity is not particularly strong as long as $\bar{e} \leqq 0.6$. The average eccentricity of the 98 known short period comets with $P < 30a$ is 0.57 (Rahe, 1981), for radio meteors (Southworth and Sekanina, 1973) it was found to be 0.5. We therefore consider an average eccentricity of 0.5–0.6 as a reasonable estimate for the particles put into the zodiacal cloud and limit ourselves in the following sections to only use the Rayleigh distribution with maximum at $e=0.5$, $h^i(e) \sim e \cdot \exp(-2e^2)$.

The influence of eccentricity was also tested for other spatial input distributions. It gets more pronounced for steeper spatial input distributions and weaker for more extended source regions. For most of the following calculations the latter effect is dominating.

b) Influence of the source distribution of semimajor axes

As a starting case we considered a source distribution where the semimajor axes are evenly distributed between 0.05 AU and 4 AU. The slope of the resulting spatial distribution was close to the observed power law between 0.4 AU and 1 AU, but too flat closer to the Sun and too steep outside 1 AU. In order to obtain a spatial distribution $n(r) \sim r^{-1.3}$ in the inner solar system, the input in this region has to be increased. Similarly, the strong decrease of spatial density towards 4 AU only can be avoided by extending the source region beyond that limit.

For circular orbits, in steady-state, the Poynting-Robertson-effect leads to spatial densities at different distances r_1 and r_2, the ratio of which is simply given by $n(r_1)/n(r_2) = (r_2/r_1)x$ (number of particles injected outside r_1/number of particles injected outside r_2). For eccentric orbits we expect the same qualitative behaviour. Therefore, the more extended the source region, the steeper a

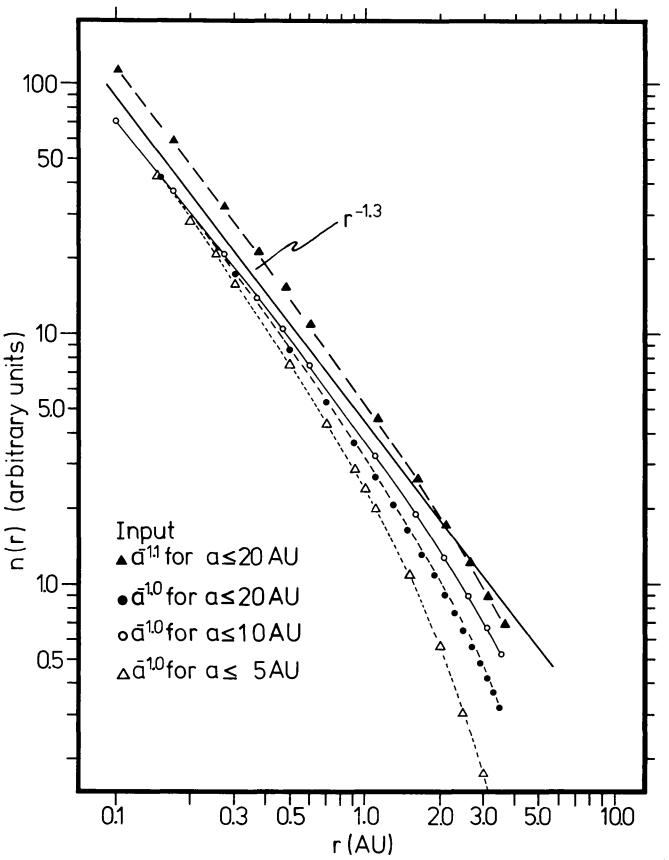

Fig. 8. Spatial distribution resulting for a source concentrated towards the Sun with a distribution $a^{-x} \cdot e \cdot \exp(-2e^2)$

distribution of semimajor axes is required. For a distribution $f^i(a) \sim a^0$, an upper limit of $a=4$ AU gives an, although very rough, approximation to the desired spatial distribution; for $f^i(a) \sim a^{-0.5}$ an upper limit of 5–10 AU (compare Fig. 7) is preferable, for $f^i(a) \sim a^{-1.0}$ limits of 10–20 AU are acceptable, while a limit of only 5 AU in this case leads to too steep a spatial distribution (Fig. 8). As mentioned in the preceding section, $f^i(a) \sim a^{-1.3}$ if the source region extends to infinity.

From the purely parametric models discussed so far the ones with $f(a) \sim a^{-1.0}$ or $a^{-1.1}$ and a source region extending out to 20 AU give the best representation of the data. In case of the latter model a mass input of $170\,\mathrm{kg\,s^{-1}}$ outside 1 AU is needed to reproduce the size distribution of Giese and Grün (1976), while the total input outside 0.1 AU is $390\,\mathrm{kg\,s^{-1}}$.

We do not want to put much weight on the selection of a "best" model because the choice may not be unique. However, two general features appeared in all models which reasonably approximated the observations: a large fraction, about half of the input occurred inside the earth's orbit ($a=0.1-1$ AU), and still about one fourth of the particles delivered had semimajor axes larger than 4 AU (Table 1). Thus the observations require both a strong source of particles near the Sun, to ascertain a steeper increase of spatial density than $1/r$, and a source extended well beyond the asteroid belt, to keep the decrease of spatial density as moderate as observed.

c) A tentative physical model

We now examine whether the input of debris from mutual collisions between interplanetary particles could lead to the

Table 1. Distribution of mass input for various models $f_1^i(a,e)=a^{-x}h^i(e)$

Model	0.1 AU $\leqq a \leqq$ 1.0 AU	$a>1$ AU	$a \geqq 4$ AU	Remark on resulting spatial distribution
a^0, $a \leqq$ 4 AU	0.3	1/per def.	0	Curved
$a^{-0.5}$, $a \leqq 10$ AU	0.3	1	0.5	Flat
$a^{-0.5}$, $a \leqq$ 5 AU	0.5	1	0.2	Curved
$a^{-1.0}$, $a \leqq$ 5 AU	1.4	1	0.1	Steep
$a^{-1.0}$, $a \leqq 10$ AU	1.0	1	0.4	Acceptable
$a^{-1.1}$, $a \leqq 20$ AU	1.0	1	0.5	Acceptable
$a^{-1.3}$, $a \leqq \infty$	1.0	1	0.7	Analytic solution
Interpretation	1	1	0.5	

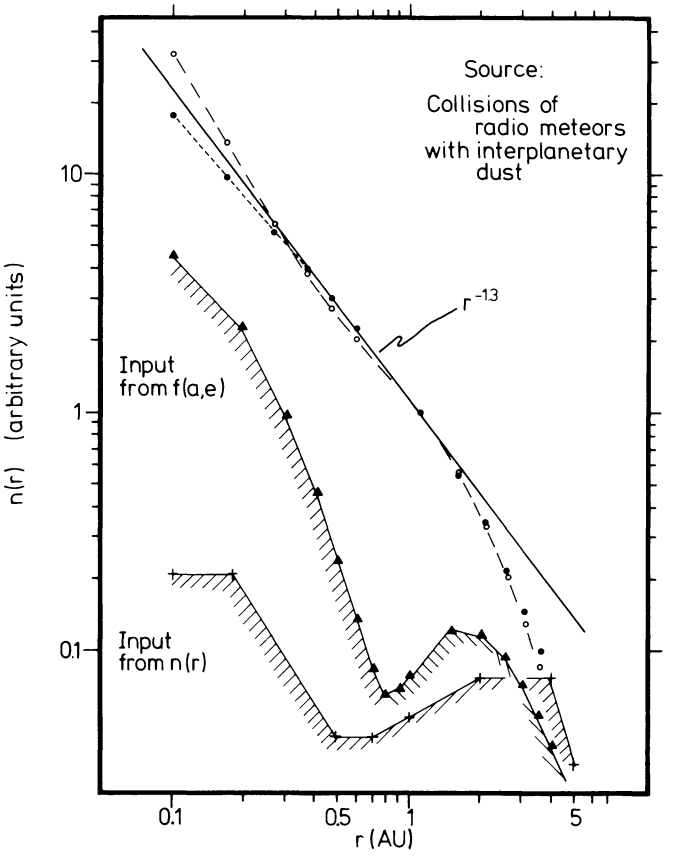

Fig. 9. Spatial distribution for particles created by collisions between radio meteors and a dust distribution $n(r) \sim r^{-1.3}$. ● Using the spatial distribution of radio meteors averaged over heliocentric ecliptic latitudes and the standard eccentricity distribution. ○ Using Southworth and Sekanina's (1973) formulae for a, e-distribution of radio meteors. The shaded curves show the radial distribution of the corresponding dust input

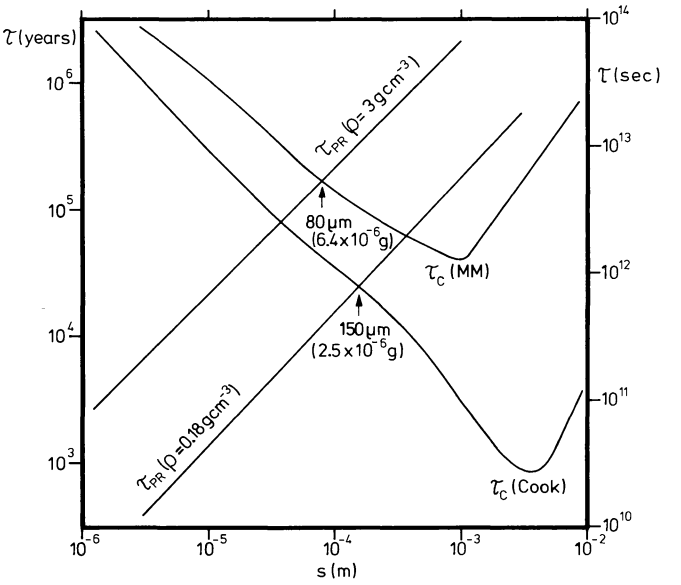

Fig. 10. Collisional lifetimes τ_c for the size distribution given by Cook (1980) with $\varrho=0.18$ g cm^{-3} and the "maximum model" of Giese and Grün (1976) with $\varrho=3$ g cm^{-3}. For comparison the Poynting-Robertson lifetimes for the appropriate densities are included. Equality between gain and loss occurs at the sizes indicated in the figure

observed relative spatial distribution. We will see in Sect. 4.4 that these collisions mainly are producing dust and destroying meteoroids. We therefore assume that we will get a reasonable estimate of the relative spatial input distribution, if we assume the targets to be distributed like meteoroids and the projectiles with the power law (19) found for interplanetary dust. The distribution of meteoroids was taken from Southworth and Sekanina (1973). We were not able to reproduce from their distribution $f_1(a,e)$ the spatial density given by these authors but obtained a stronger increase towards the Sun. Therefore we did the calculations for both resulting spatial input distributions. One results in a steeper, the other in a flatter spatial density distribution of interplanetary dust than observed. In any case there remain uncertainties in the distribution of radio meteoroids because it is based on extrapolation to unobservable orbits. Within these uncertainties Fig. 9 may be considered an acceptable result. We conclude from this that radio meteoroids are a possible source of interplanetary dust, provided it may be shown that the dust input resulting from the disruption of meteors is sufficient to maintain the interplanetary dust cloud.

4.3. *The effect collisional losses on the spatial distribution*

Using our collisional model (Sect. 2.3) collisional lifetimes were calculated for values of the parameter Γ between 10^3 and 10^6. Simulation experiments as summarized by Grün (1981) favour a value of Γ near $5\,10^4$. Collisional lifetimes for this value are shown in Fig. 10, for the size distribution given by Giese and Grün (1976)

as well as for that of Cook (1978). We note that Cook's size distribution, which appears too high to us, gives essentially the same result as obtained by Dohnanyi (1978), who therefore also may tend to overestimate the influence of collisions. As argued in Sect. 2.2, we prefer the size distribution of Giese and Grün. In Fig. 11 we summarize the values of the ratio τ_{PR}/τ_c obtained for their "maximum model". The results are in good agreement with the values of Zook and Berg (1975) who calculated the probability of catastrophic collisions when a particle drifts from 1 to 0.1 AU. Transformation to values of τ_{PR}/τ_c was accomplished using (27). There is a discrepancy to Dohnanyi's (1978) values which are one to two orders of magnitude higher. This is the result of the much higher number density he uses.

In order to select a range of values of τ_{PR}/τ_c appropriate for the zodiacal cloud we note that the maximum contribution to the zodiacal light per logarithmic size interval occurs near 30 μm radius, 60% of the light being contributed by particles with $10\,\mu m \leqq s \leqq 60\,\mu m$. As probable range for Γ we select $10^4 - 5\,10^4$, the former value being preferred in a recent study of Le Sergeant d'Hendecourt and Lamy (1981). Inspection of Fig. 11 shows that $\tau_{PR}/\tau_c = 0.1$–0.3 are reasonable values for the particles producing the zodiacal light. The smaller of these values corresponds to a survival probability of 50% for a particle drifting from 4 AU to 0.1 AU (Fig. 2). The effect of collisions on the lifetime of interplanetary dust particles therefore is neither dominating nor negligible but intermediate.

The effect of collisions on the spatial distribution was studied by numerical calculations with different values of the parameter τ_{PR}/τ_c. An input distribution $f^i(a,e) \sim a^{-1.1}$ up to distances of 10 AU from the Sun was chosen, which gives a reasonable fit to the $r^{-1.3}$ law for low collisional losses ($\tau_{PR}/\tau_c = 0.1$). The left part of Fig. 12 already shows the tendency of $n(r)$ to approach the power law of the input distribution for semimajor axes if collisions become dominant ($\tau_{PR}/\tau_c \gg 1$).

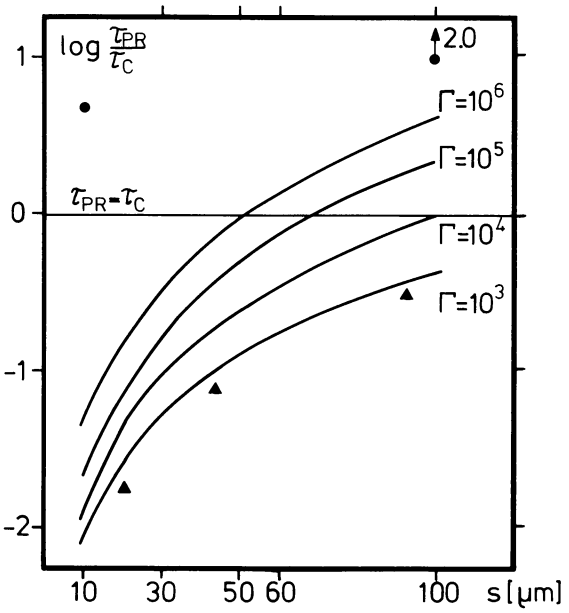

Fig. 11. The ratio of lifetimes τ_{PR}/τ_c at 1 AU as a function of particle radius s for different values of the parameter Γ. For comparison values given by Zook and Berg (1975), ▲, $\Gamma = 10^3$ and Dohnanyi (1978), ●, $\Gamma = 4\,10^5$ are included.

In order to further demonstrate this effect of collisions, the right part of the figure shows the result of calculations for the — unrealistic – case in which there are no source particles with

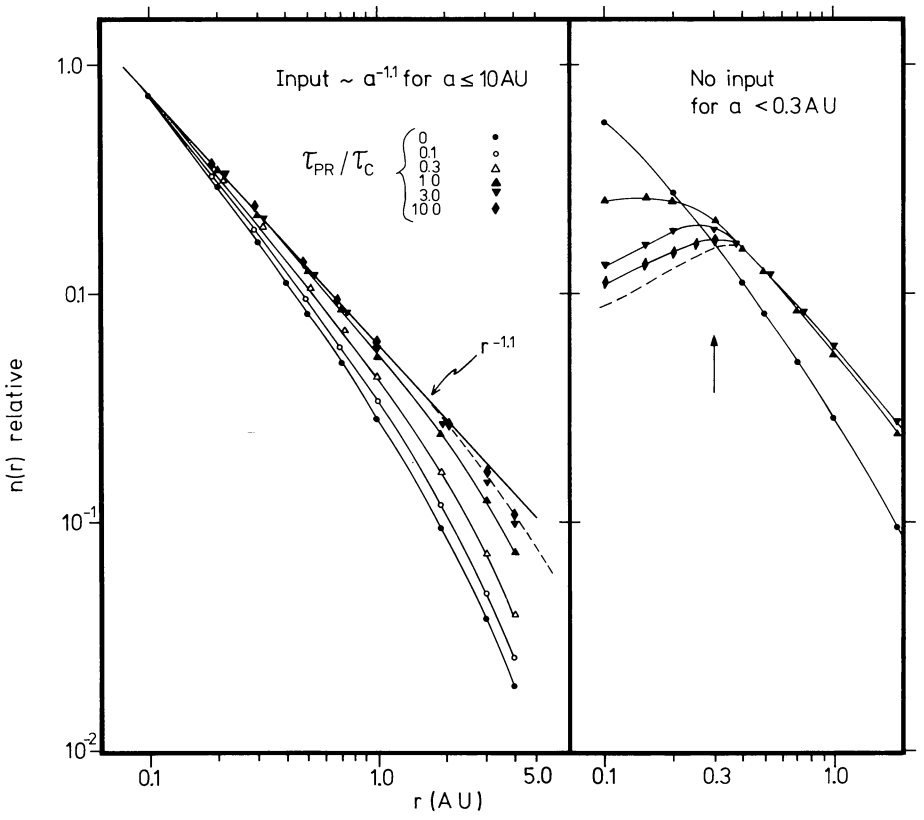

Fig. 12. Left: influence of collisions on the resulting spatial distribution of interplanetary dust for an input function $f^i(a,e) \sim a^{-1.1} \cdot e \cdot \exp(-2e^2)$, $a \leqq 10$ AU. Right: same, but no input for $a \leqq 0.3$ AU. The broken line shows the expected limiting result for $\tau_{PR}/\tau_c \to \infty$

Table 2. Dust production rates P (kg s^{-1}) required to maintain the observed density distribution of interplanetary dust. The values refer to an input distribution $\sim a^{-1.1}$ inside 10 AU (Fig. 12), except the last model which was chosen $\sim a^{-1.27}$ to fit the observed spatial distribution

$\frac{\tau_{pr}}{\tau_c}$	P (0.1 AU $\leqq a \leqq$ 1 AU)	P ($a \geqq$ 1 AU)	P (total)
0	260	210	470
0.1	310	250	560
0.3	440	350	790
1	980	780	$1.8\,10^3$
3	$2.8\,10^3$	$2.2\,10^3$	$5.0\,10^3$
10	$9.2\,10^4$	$7.3\,10^3$	$1.7\,10^4$
1	1400	750	$2.2\,10^3$

$a < 0.3$ AU. Whereas without collisions the missing input is hardly detectable, the input distribution is clearly approximated for $\tau_{PR}/\tau_c \gg 3$. The production rates which are required to maintain a steady-state distribution of interplanetary dust with densities at 1 AU as given by Giese and Grün (1976), were evaluated for the left part of Fig. 12. Results are shown in Table 2. As expected, the required production rate strongly increases when collisional losses become important. In absence of collisions for this model an input of 470 kg s^{-1} outside 0.1 AU is required. This is 20% more than for the model of Fig. 8, because there the source region is more extended with the result that at 1 AU average eccentricities and drift velocities are somewhat smaller. But equality of the times scales, $\tau_{PR}/\tau_c = 1$, already leads to a four times higher required production rate. Also a comparison with the last model of Table 2, which also was chosen to fit the observed spatial distribution, shows that if collisions are important a larger fraction of the dust production has to occur inside 1 AU.

4.4. *Dust production by collisions*

Above we mentioned that collisions between radio meteoroids and dust particles would provide an input leading to an acceptable relative spatial distribution of interplanetary dust. However, we still have to show that radio meteoroids, which we considered a possible source of dust supply, are able to account *quantitatively* for the required mass input. The basis of our analytical calculation was application of the collisional model to the known size distribution of interplanetary particles at 1 AU. This yields size-dependent rates of loss and gain according to Eqs. (15) and (16) which are shown in Fig. 13. The resulting dust production rate ($1.4\,10^{-32}$ kg/m^3 s for Giese and Grün's (1976) maximum model, $1.1\,10^{-30}$ kg/m^3 s of Cook's (1978) size distribution easily can be integrated over the planetary system under our assumption of a distance-independent size distribution for a given spatial distribution. The filling factor resulting from the concentration of dust to the ecliptic plane is found to be 0.23, based on the dust distribution

$$n(r, z)/n(r, 0) = \exp(-2.1 \cdot |z/r|), \tag{35}$$

which gives a good representation of the Helios zodiacal light observations (Leinert, 1980).

The results are summarized in Table 3. Figure 13 shows that collisions mainly lead to the production of dust ($s \leqq 100$ μm) at the expense of the larger meteoroids ($m \geqq 10^{-5}$ g).

5. Discussion

5.1. *Relative spatial distribution*

Our present knowledge of solid interplanetary particles implies that inevitably mutual collisions provide a sizeable continuous input to the interplanetary dust cloud over a large part of the planetary system. Models relying on an isolated source of dust particles therefore are considered artificial. In addition, they also poorly represent the observations.

For example, occasionally the Asteroid Belt has been discussed as direct source of interplanetary dust (Gillett, 1966). The particle orbits then would be of low eccentricity. From Fig. 5 we see that in this case the resulting spatial distribution would be too flat, $n(r) \sim 1/r$. Also the figure shows that a depletion rather than an enhancement of dust in the Asteroid Belt has to be expected under the action of the Poynting-Robertson-effect. A steeper spatial distribution could be obtained with an isolated source if the particles initially were in eccentric orbits, but then the distribution would be too steep at large, too flat at small heliocentric distances (Fig. 5). This means that short period comets ($P < 30a$), of which 68% are concentrated to semimajor axes between 3 AU and 4 AU, by themselves also are no adequate direct source for interplanetary dust.

Trulsen and Wikan (1980) suggested an external isolated source, but with inelastic collisions decreasing the average inclination of the dust particles during their drift towards the Sun. This procedure is able to explain to observed radial distribution of interplanetary dust in the ecliptic. It is not clear, however, whether the gradual change of momentum by collisions also would work if the particles are destroyed by collisions, as typically is the case in interplanetary space. The predictions of Trulsen and Wikan are also not compatible with the zodiacal light observations. First, their mechanism requires the inclinations to be Rayleigh-

Table 3. Mass input (kg s^{-1}) into the interplanetary dust cloud ($s \leqq 100$ μm) from destructive collisions ($\Gamma = 5\,10^4$)

Size distribution	Spatial distribution		
	$n \sim r^{-1.3}$	n (radio meteoroids) from Southworth and Sekanina	Projectiles: $n \sim r^{-1.3}$ targets: n (radio meteoroids)
Giese and Grün ("maximum model")	200	4,400	1,200
Cook	13,000	270,000	73,000

distributed. This results in a decrease of dust density outside the ecliptic proportional to $\exp(-\gamma z^2/r^2)$, leading to a decrease of zodiacal light intensity which is slower than observed near the ecliptic (Leinert et al., 1976) and stronger than observed in the helioecliptic meridian at ecliptic latitudes 15°–30°. Second, the predicted strengthening of the brightness concentration to the ecliptic at small heliocentric distances ($\gamma \sim 1/r^{0.3}$) is not observed (Leinert et al., 1981), and the interpretation of the two-dimensional zodiacal light distribution rather requires a decreasing relative scale height of the dust distribution for *larger* heliocentric distances.

We therefore come back to the existence of an extended source region as a natural explanation for the radial distribution of interplanetary dust. According to our models which neglect collisional losses, e.g. Fig. 8, the mass input required to balance the loss due to the Poynting-Robertson-effect is about 400 kg s^{-1} if we assume an average eccentricity of the particle orbits of $e \approx 0.5$. About half of this material is needed in the region 0.1–1 AU, and about a quarter of it has to be outside 4 AU. We now discuss the influence of eccentricity and collisions on this basic result. Sputtering was found to be unimportant. A moderate eccentricity of $e \approx 0.5$ is valid for radio meteors and similar values of $e = 0.6$–0.7 were found for dust particles in the mass range 10^{-12} g–10^{-9} g (Grün, 1981). Nevertheless we want to note that larger eccentricities would lead to an increase in the required mass input outside 1 AU. At 0.1 AU virtually no effect remains because there the average eccentricity gets rather small, while the particles are drifting so close to the Sun.

The effect of collisions mainly is to increase the required mass input, e.g. in case of the model shown in Fig. 12 from 470 kg s^{-1} to 560 kg s^{-1} for $\tau_{PR}/\tau_c = 0.1$ and to 1800 kg s^{-1} for $\tau_{PR}/\tau_c = 1.0$. The relation between source distribution and resulting steady-state spatial distribution also is affected, but not substantially. Indeed, if collisions completely determine the lifetime of interplanetary dust particles, an input distribution $f^i(a)$ simply translates into a spatial distribution $n(r) \sim f^i(r)$, the same relation as obtained in the absence of collisions for a very extended source region and for a power law $f^i(a) = a^{-x}$ with $x > 1$. Of course, if destructive collisions are very frequent, little can be said on the source outside the heliocentric distance of the observer. The farthest observations reported so far are the particle detections of Humes (1980) out to 18 AU. *Assuming* a power law distribution $a^{-1.3}$ for the input source out to 20 AU, under strong collisions 63% of the mass input would have to occur inside 1 AU, 10% outside 4 AU. This is not very different from the results neglecting collisional losses.

In addition, destructive collisions are expected to change the size spectrum. Assuming the size spectrum of the input material to be the same everywhere, the larger destruction rate for larger particles would reduce their number closer to the Sun. The order of the effect may be judged from Fig. 12, where between 1 AU and 0.1 AU the reduction factor is 20% for $\tau_{PR}/\tau_c = 0.1$, a factor of 1.9 for $\tau_{PR}/\tau_c = 1.0$, when compared to the case without collisions. Based on Fig. 11 this would affect significantly only particles larger than 50–100 μm in radius, and therefore is difficult to verify by zodiacal light or particle detection experiments, because these large particles are rare and their optical properties are at most weakly size dependent. Strictly speaking, the relative spatial distribution (30) then no longer is independent of size which has to be taken into account for a fully self-consistent treatment. As the effect is not dramatic, and since our emphasis is on the spatial rather than the size distribution we continue our discussion without referring to these size effects.

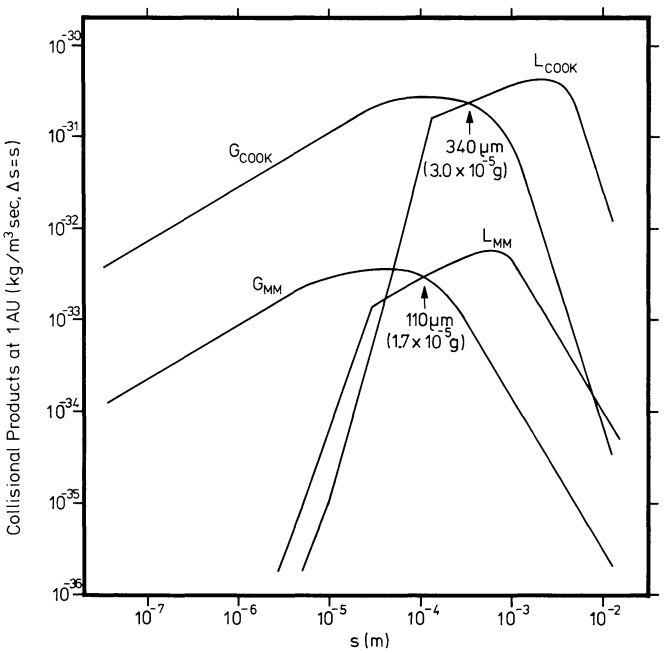

Fig. 13. Loss (L) and gain (G) of particles at 1 AU in the ecliptic according to our collisional model. The calculations were performed with $\Gamma = 5\,10^4$ for the size distributions of Giese and Grün (MM, 1976) and Cook (1978)

The discussion so far emphasizes that our explanation for the *relative* spatial distribution is acceptable, i.e. we do need an extended source region with large part of the input inside 1 AU and still a considerable contribution outside 4 AU. We have shown in Fig. 9 that mutual collisions of interplanetary particles could give the correct relative spatial distribution. We still have to show that this source also would be able to account quantitatively for the required dust input.

5.2. *Mass balance*

The mass loss of the interplanetary dust cloud outside 0.1 AU was found to be 400–800 kg s^{-1} for models with no or only a moderate importance of collisions, $\tau_{PR}/\tau_c = 0.1$–0.3. However, we have to keep in mind that our procedure overemphasizes the effect of collisions. Mukai and Yamamoto (1982) calculated the contribution of solar wind to the Poynting-Robertson-effect. Dust particles are in prograde orbits (James and Smeethe, 1970), but due to an error in sign one has to use Mukai and Yamamoto's calculations for retrograde orbits. This leads to a decrease of τ_{PR} and consequently τ_{PR}/τ_c by a factor of 1.5, which we did not consider so far, and to an increase in the Poynting-Robertson loss rate by the same amount. The amount of collisions essentially would remain constant, giving a total dust loss rate of 600–1000 kg s^{-1}. Below we will come back to the point that colliding particles are not completely lost, but their material partly reappears at smaller sizes. However, our present discussion of balance remains untouched by this point. The required amount of dust could easily be provided by collisions, if the size distribution of Cook (1978) were used. But we stated earlier that his spatial densities appear too high to us. On the other hand, the dust production on the basis of Giese and Grün's size distribution is only 200 kg s^{-1} for a spatial distribution $n \sim r^{-1.3}$.

However, we do not consider this a serious problem. This size distribution in its absolute value is determined hardly better than by a factor of two. A revision of spatial density by a factor of two upward as advocated by Hanner (1980) from a comparison with zodiacal light brightnesses would increase dust production by a factor of four. Also it has to be noted that the result is sensitive to the spatial distribution of dust and meteoroids outside 1 AU. Should both populations follow the distribution of Southworth and Sekanina (1973), which, however, we consider unlikely, the input would rise to over 4000 kg s^{-1}. If only the meteoroids showed the enhanced density in the asteroid belt typical of Southworth and Sekanina's results, then still a dust production of about 1000 kg s^{-1} is expected. While details of the meteoroid distribution are quite uncertain, Cook (1978) makes a strong case that at least the qualitative features of Southworth and Sekanina's result are correct. It is therefore not unreasonable to assume that the main part of the required dust supply is taken from the background of meteoroids by collisions, mostly with dust particles. Only a small fraction appears and needs to be injected *directly* by comets.

5.3. *Mass loss from interplanetary space*

The Poynting-Robertson-effect introduces a true mass loss. The collisional losses appearing in Table 2, however, partly are counterbalanced by the smaller dust particles created during collisions. Only this fraction of the mass involved in a collision is truly lost, which is converted to particles of such a small size that they are blown out of the planetary system by radiation pressure. We take the limiting size for stability against radiation pressure to be 1 μm. On the basis of our calculations, for the size distribution of Giese and Grün, then 50% of the calculated loss by collisions for dust particles ($s \leqq 100$ μm) actually is lost from interplanetary space. This leads to a true mass loss of about 800 kg s^{-1} outside 0.1 AU.

Our value is similar to the findings of Le Sergeant d'Hendecourt and Lamy (1981) who calculated the size and number of collisional fragments for a size distribution derived in an earlier paper (Le Sergeant d'Hendecourt and Lamy, 1980), which is not very different from Giese and Grün's. Their outward flux of β-meteoroids of $4.0\,10^{-22}$ g cm^{-2} s^{-1} with (35) translates into a loss of 470 kg s^{-1} inside 1 AU, which is of the same size as our result.

Earlier investigations (Dohnanyi, 1972; Whipple, 1967) estimated the mass loss for the cloud of interplanetary particles to be much higher, 10–30 10^3 kg s^{-1}. Whipple also finds that the losses due to Poynting-Robertson-effect alone would be of the order of 10^3 kg s^{-1}. He calculates the total mass loss from the total mass of the cloud of interplanetary particles, estimated to be $2.5\,10^{19}$ g, and an average lifetime of about 10^5 yr, assuming that 30% of the mass involved in a collision is immediately converted to β-meteoroids. Because his mass of the interplanetary cloud is 20 times higher than in our model with $n(r) \sim r^{-1.3}$, and because he adds an additional factor of three (to obtain the short lifetime required to understand the existence of streams in photographic meteors), the reason for his high resulting losses can be qualitatively understood. Dohnanyi also starts from the total mass of interplanetary particles given by Whipple, for which his collisional model results in a mass loss of about 25 10^3 kg s^{-1}. While the details of these calculations are not easy to follow, such a number may be expected on the basis of the higher spatial density of particles he uses. From Fig. 11 we conclude that his collisional lifetimes correspond to $\tau_{PR}/\tau_c \approx 10$ in the range of radii 10 μm–60 μm, which dominates the zodiacal light. Table 2 shows that for such short lifetimes a high production rate of the order of 20 10^3 kg s^{-1} is required, because a high loss occurs. Nevertheless it is worthwhile to clarify the discrepancy to our predicted true mass loss of 800 kg s^{-1} on the basis of a critical discussion of size and spatial distribution of interplanetary particles.

Present short period comets would not be able to supply even this moderate amount. The estimate of 70–250 kg s^{-1} (Delsemme, 1976; Röser, 1976) may have been optimistic, since detailed studies (Sekanina and Schuster, 1978) resulted in an average product of albedo and dust production of only 200 g s^{-1} for comet Encke. This presents a difficulty only of one requires the dust particles to be injected directly by comets. If on the other hand dust is mainly being produced from a reservoir of long-lived larger particles by collisions there is no need to balance the mass losses on a short timescale.

5.4. *Average inclination*

It may be noted, that the orbital inclination ($\bar{i} = 17°$) also places radio meteors at a position intermediate between short period comets ($\bar{i} = 13°$ for $P < 30a$) and interplanetary dust ($\bar{i} = 30°$). As earlier (Leinert et al., 1976) we take this as an additional indication that radio meteors could represent the immediate source of interplanetary dust.

6. Conclusion

From our attempt to explain the observed spatial distribution of interplanetary dust the following picture emerges:

a) There is a primary source of solid particles (comets?) which, apart from delivering some dust directly, mainly

b) fills the reservoir of (radio) meteoroids.

c) From this reservoir a continuous input of $\geqq 200$ kg s^{-1} to the interplanetary dust cloud is created by catastrophic collisions, mostly with dust particles, which reduces the size of the reservoir particles.

d) The spatial distribution of the input over the resulting extended source region, by action of the Poynting-Robertson-effect, leads to the observed spatial distribution of dust within the limits of uncertainty in the spatial distribution of meteoroids.

e) Collisions of the dust particles constitute a loss mechanism in addition to the Poynting-Robertson-effect, but have little influence on the resulting spatial distribution. For plausible average values of collision liefetimes, $\tau_{PR}/\tau_c = 0.1$–0.3, the required mass input of 600–1000 kg s^{-1} probably is available from the reservoir.

Acknowledgements. One of us (J. Buitrago) thanks the Max-Planck-Institut für Astronomie for its hospitality during the larger part of the work on this paper.

We thank H. Elsässer, E. Grün, H. Zook, and T. Mukai for stimulating discussions. The computations were performed at the computing centers of the Max-Planck-Institut für Kernphysik and of the Universität Heidelberg.

References

Bandermann, L.W.: 1967, Thesis, Univ. of Maryland
Briggs, R.E.: 1962, *Astron. J.* **67**, 710
Cook, A.F.: 1978, *Icarus* **33**, 349

Delsemme, A.H.: 1976, *Lecture Notes Phys.* **48**, 314
Dohnanyi, J.S.: 1972, *Icarus* **17**, 1
Dohnanyi, J.S.: 1978, in *Cosmic Dust*, ed. J.A.M. McDonnell, Wiley, Chichester, New York, Brisbane, Toronto, p. 527
Fechtig, H., Leinert, C., Grün, E.: 1981, in *Landolt-Börnstein, New Series*, Group VI, Vol. 2a, eds. K. Schaifers and H.H. Voigt, Springer, Berlin, Heidelberg, New York, p. 232
Fujiwara, A., Kamimoto, G., Tsukamoto, A.: 1977, *Icarus* **31**, 277
Giese, R.H., Grün, E.: 1976, *Lecture Notes Phys.* **48**, 135
Gillett, F.C.: 1966, Thesis, Univ. of Minesota
Grün, E.: 1981, Habilitationsschrift, Univ. Heidelberg
Grün, E., Fechtig, H., Kissel, J., Gammelin, P.: 1977, *J. Geophys.* **42**, 717
Hanner, M.S.: 1980, *Icarus* **43**, 373
Hanner, M.S., Sparrow, J.G., Weinberg, J.L., Beeson, D.E.: 1976, *Lecture Notes Phys.* **48**, 29
Haug, U.: 1958, *Z. Astrophys.* **44**, 71
Hawkins, G.S., Southworth, R.B.: 1961, *Smithonion Constr. Astrophys.* **4**, 85
Humes, D.H.: 1980, *J. Geophys. Res.* **85**, 5841
James, J.F., Smeethe, M.J.: 1970, *Nature* **277**, 588
Leinert, C., Link, H., Pitz, E., Giese, R.H.: 1976, *Astron. Astrophys.* **47**, 221
Leinert, C., Hanner, M., Richter, I., Pitz, E.: 1980, *Astron. Astrophys.* **82**, 328
Leinert, C., Richter, I., Pitz, E., Planck, B.: 1981, *Astron. Astrophys.* **103**, 177
Leinert, C., Richter, I., Pitz, E., Hanner, M.: 1982, *Astron. Astrophys.* **110**, 355
McDonnell, J.A.M., Ashworth, D.G., Carey, W.C.: 1980, *Planetary Space Sci.* **28**, 625
Mukai, T., Yamamoto, T.: 1982, *Astron. Astrophys.* **107**, 97
Rahe, J.: 1981, in *Landolt-Börnstein, New Series*, Group VI, Vol. 2a, eds. K. Schaifers and H.H. Voigt, Springer, Berlin, Heidelberg, New York, p. 202
Robertson, H.P.: 1937, *Monthly Notices Roy. Astron. Soc.* **97**, 423
Röser, S.: 1976, *Lecture Notes Phys.* **48**, 319
Röser, S., Staude, H.J.: 1978, *Astron. Astrophys.* **67**, 381
Schuerman, D.W.: 1980, in *Solid Particles in the Solar System, Proc.* IAU *Symp.* **90**, eds. I. Holliday and B.A. McIntosh, Reidel, Dordrecht, Boston, London, p. 71
Sekanina, Z., Schuster, H.E.: 1987, *Astron. Astrophys.* **68**, 429
Le Sergeant d'Hendecourt, L.B., Lamy, Ph.L.: 1980, *Icarus* **43**, 350
Le Sergeant d'Hendecourt, L.B., Lamy, Ph.L.: 1981, *Icarus* **47**, 270
Southworth, R.B.: 1967, in *The Zodiacal Light and the Interplanetary Medium*, ed. J.L. Weinberg, NASA SP-150, Washington, p. 257
Southworth, R.B., Sekanina, Z.: 1973, NASA Contract Report CR-2316, Washington
Trulsen, J., Wikan, A.: 1980, *Astron. Astrophys.* **91**, 155
Whipple, F.L.: 1967, in *The Zodiacal Light and the Interplanetary Medium*, ed. J.L. Weinberg, NASA SP-150, Washington, p. 409
Wyatt, St.P., Jr., Whipple, F.L.: 1950, *Astrophys. J.* **111**, 134
Zook, H.A., Berg, O.E.: 1975, *Planetary Space Sci.* **23**, 183